



Regional climate model RCA4 simulations of temperature and precipitation over the Arabian Peninsula: sensitivity to CORDEX domain and lateral boundary conditions

F. S. Syed¹ · M. Latif² · A. Al-Maashi¹ · A. Ghulam¹

Received: 17 March 2019 / Accepted: 4 September 2019 / Published online: 11 September 2019
© Springer-Verlag GmbH Germany, part of Springer Nature 2019

Abstract

Regional Climate Models (RCMs) are increasingly used to add small-scale processes at higher grid resolution that are not represented by their Lateral Boundary Conditions (LBCs). Rossby Centre regional atmospheric model, RCA4, has down-scaled three Global Climate Models (GCMs), namely, CNRM-CM5, EC-EARTH and GFDL-ESM2M in the COordinated Regional climate Downscaling EXperiment (CORDEX) framework for Middle East North Africa (MENA) and South Asia (SA) domains. Arabian Peninsula is covered in both MENA and SA simulations, which gives a unique opportunity to study the effects of CORDEX domain and LBCs on the simulation of temperature and precipitation by RCM. It is examined by calculating the differences between MENA and SA simulations for different driving GCMs in the historical (1976–2005) and future (2071–2100) periods under RCP8.5 emission scenario, for both summer (dry) and winter (wet) seasons. RCA4 performs generally well when simulating the observed temperature and precipitation patterns, with some local wet biases over Asir Mountains and cold bias over the north eastern parts of Saudi Arabia. The simulations of temperature seem to be very sensitive to the simulation domain (i.e., MENA and SA) and less sensitive to different LBCs, whereas in case of precipitation LBCs seems to play a dominant role. The MENA simulations generally project about 2 °C warmer and drier climate compared to SA simulations by the end of this century, which is comparable to the differences arising due to different LBCs and climate change.

Keywords Arabian Peninsula · Temperature · Precipitation · Domain · Lateral boundary conditions · Sensitivity · RCM · CORDEX

1 Introduction

Unmatched changes in climate have been observed since 1950s at different spatial and temporal scales and climate change has become one of the major challenges that the world is facing, as highlighted in the Fifth Assessment Report (AR5) of the Intergovernmental Panel on Climate Change (IPCC 2013). Warmer atmosphere and oceans, reduction in snow and ice cover over the mountains and

poles, and the rise in sea level have been observed globally with regional variations due to increase in the atmospheric greenhouse gases (GHGs) concentration. Climate change is affecting many aspects of our daily life, especially after the industrial revolution. It has become crucial to study the projected changes in the climate in order to study multi-disciplinary impacts of climate change. Arabian Peninsula (AP) has generally desert climate, which is characterized by extremely high (cool) temperatures during day (night) time. The amount of annual rainfall in the AP is low and erratic, except in the areas of the Asir Mountains on south-western coast of AP which receives an average of 300 mm annually. The main synoptic feature is the sub-tropical high pressure area prevailing over the region, causing significant variations in the temperature and humidity. The rainfall in this arid region is mainly governed by its topography (Lioubimtseva 2004). Evans (2009) analyzed 18 Global Climate Models (GCMs) data and found that Middle East region is likely to

✉ F. S. Syed
faisal.met@gmail.com

¹ General Directorate of Climate Services, The General Authority of Meteorology and Environmental Protection (GAMEP), Jeddah 21577, Kingdom of Saudi Arabia

² Department of Meteorology, COMSATS University Islamabad (CUI), Islamabad 45550, Pakistan

experience an increase of 1.4 °C in the mean temperatures in middle of the twenty-first century, which is likely to increase further to touch 4 °C by the end of this century. Almazroui et al. (2017) also studied the uncertainties in projected temperature and precipitation over the AP. The total amount of precipitation over the Middle East was also predicted to decrease in the winter season because of weakening of the eastern Mediterranean storms (Evans 2009, 2010). Severe water shortage is expected over the Middle East North Africa (MENA) region due to significant decreasing trend in the rainfall, as examined by Sowers et al. (2011) using global climate change models. Other climate indicators, i.e., increased number of warm days and decreased frequency of cold days, have shown clear warning signal (Zhang et al. 2005) in the Middle East region.

Main features of present-day climate are generally well simulated by the GCMs at different spatial and temporal scales (Houghton et al. 2001). Climate change projections of temperature and precipitation produced by GCMs are widely used to study the climate change impacts on different socio-economic sectors of life and different mechanisms of the climate system itself. Dynamical modeling of climate for long-term basis is computationally expensive practice. This brings in the usage of Regional Climate Models (RCMs) as a common method to obtain fine-scale regional climate information by dynamical downscaling the GCMs outputs. RCMs can better resolve atmospheric fields because of their higher spatial resolution, which makes it possible to represent small-scale physical processes (e.g., extreme precipitation events, coastline effects, heterogeneity in land cover, mountain-related circulations effects, meso-scale cyclones and related weather phenomena). Higher resolution topography and land-surface characteristics are incorporated in RCMs and these features then interact with the model atmosphere which results in better representation of precipitation especially for the mountainous regions (Feser et al. 2011). RCMs have been extensively used in recent years for diagnostic studies and climate change (Bozkurt and Sen 2011; Messenger et al. 2004). Apart from the biases in RCMs associated with LBCs, initial conditions, numerical algorithms, surface forcing and model physics (Wu et al. 2005); enhanced resolution can also add errors and uncertainties in reproducing regional climate. In this regard, the uncertainties related to RCMs need to be accounted for in studying climate change impact on different socio-economic sectors, such as water resources, agriculture and health (Bergant et al. 2007). Many studies have focused on the past and future climate projections using RCMs (e.g. Pal and Eltahir 2016; Buchignani et al. 2018; Almazroui et al. 2013; Almazroui 2013). Pal and Eltahir (2016) suggested that future temperature in south-west Asia may exceed a threshold for human adaptability.

The RCMs sensitivity to the selection of simulation domain and Lateral Boundary Condition (LBC) has

remained the part of discussion in the scientific literature (e.g., Jones et al. 1995, 1997; Jacob and Podzun 1997; Denis et al. 2003; Leduc and Laprise 2009; Colin et al. 2010). Shiao and Juang (2006) showed that the large-scale atmospheric circulation and rainfall distribution are more sensitive to domain size compared to horizontal resolution of the RCM. Almazroui (2012, 2016) conducted domain size experiments and concluded that the simulation of precipitation events across the AP is influenced by the size of domain. He found that, only increasing resolution of RCM does not improve the simulation of precipitation events unless there is a clear signal in the driving forcings. The smaller domain gives a better representation of observed precipitation, however in the larger domain the precipitation sensitivity to initial soil moisture is more realistic (Seth and Giorgi 1998). They concluded that the careful selection of RCM domain is very important and a larger domain should be selected compared with the area of interest for the study of internal forcings sensitivity. The domain within an RCM must be large enough to avoid an unrealistic response to internal forcings and for the full development of fine-scale features (Giorgi and Mearns 1999; Jones et al. 1995). However, Centella-Artola et al. (2015) found that the three different domain configurations over the Caribbean region using the PRECIS regional climate model show more similarities than differences in the simulated results. Wu et al. (2005) investigated the uncertainties associated with the initial conditions and lateral boundary forcing in the fifth-generation non-hydrostatic Mesoscale Model (MM5). The initial and LBCs were prepared using four widely used different global reanalysis products to determine the spread of bias as a source of uncertainty in the model simulations. Their results indicate that the difference among global datasets contribute significantly to the uncertainties in the ensemble experiments. The sensitivity and response of RCM to uncertainties employing random perturbation approach in both initial conditions and lateral inflow was examined by Giorgi and Bi (2000). They found the largest response in summer season. Using the Big-Brother Experiment (BBE) framework, Diaconescu et al. (2007) investigated the response of a RCM to errors in the driving data based on the impact of the lateral forcing and found nearly linear dependence relation between large-scale errors in RCM and in the driving data. Based on BBE framework, Denis et al. (2002, 2003), Antic et al. (2004), and Dimitrijevic and Laprise (2005) further showed that the RCM has the capability to reproduce well the small-scale climate statistics for summer and winter seasons over the different regions with different orographic forcing.

COordinated Regional climate Downscaling EXperiment (CORDEX) is the World Climate Research Program (WCRP) initiative. In this project 5th Coupled Model Intercomparison Project (CMIP5) GCM simulations (Taylor et al. 2012) are downscaled using different RCMs for the

recent historical past and twenty-first century, over most of the regions on the globe for different GHGs concentration scenarios. These RCM simulations cover most of the uncertainties associated with regional climate. The Middle East North Africa (MENA) and South Asia (SA) CORDEX Program is the branch of the International CORDEX program for the assessment of impacts of climate change over the Arab and south Asia regions, respectively on different socio-economic sectors. AP is covered in both the MENA and SA CORDEX simulations (Fig. 1). Here we study the sensitivity of COREDX domain and driving GCMs on the simulation of temperature and precipitation by RCM. Therefore, the objective of the present paper stands on the following research questions: (1) How well the RCM RCA4 is simulating temperature and precipitation over the AP with ERA-Interim (hereafter ERAINT) boundary conditions in both MENA and SA simulations? (2) How much is the difference between MENA and SA simulations, i.e., domain sensitivity? (3) What is the effect of LBCs, forced by ERAINT and different GCMs, on the simulation of temperature and precipitation over the AP (i.e., sensitivity to driving global

fields) for both summer and winter seasons? (4) What is the effect of different CORDEX domains and LBCs on the climate change scenarios of temperature and precipitation for the twenty-first century?

The structure of the present paper is organized as follows: Sect. 2 represents the data description of observed and climate models along with the statistical methods used. The results and discussions are presented in Sect. 3, which include the RCA4 model verification using ERAINT reanalysis dataset and global climate models CNERM-CM5, EC-EARTH and GFDL-ESM2M as a forcing data for both MENA and SA simulations. This section further addresses the analysis of domain and LBCs sensitivity for the historical period and its effects on the twenty-first century climate change scenarios. Finally, the summary and major conclusions of this study are presented in Sect. 4.

2 Data and methods

2.1 Observational and reanalysis datasets

Mean of five different observational temperature and precipitation datasets are used in this study for the evaluation of climate model RCA4. Multiple observational datasets are used in order to cater for observational uncertainty in this region (Tanarhte et al. 2012; Zittis 2018). The datasets are obtained from different sources: (1) University of East Anglia, UK Climate Research Unit (CRU); (2) NOAA Climate Prediction Center (CPC) global unified precipitation and temperature daily data; (3) University of Delaware (UDEL) global gridded high resolution station (land) data; (4) Global Precipitation Climatology Centre (GPCC); (5) NOAA Global Historical Climatology Network and the Climate Anomaly Monitoring System (GHCN-CAMS); (6) Potsdam Institute for Climate Impact Research, Earth2Observe, WFDEI and ERA-Interim data Merged and Bias-corrected for ISIMIP (EWEMBI). The details of these observational temperature and precipitation datasets are given in Table 1.

The ERAINT reanalysis dataset (Dee et al. 2011) at $0.5^\circ \times 0.5^\circ$ horizontal resolution of Mean Sea Level Pressure (MSLP), winds (zonal u and meridional v) and specific humidity at 850 hPa has also been used for comparison with model large-scale circulation. The ERAINT is also one of the boundary datasets for RCA4 simulation for the period 1980–2005.

2.2 Model datasets

The Rossby Center RCM RCA is developed at the Swedish Meteorological and Hydrological Institute (SMHI). The fourth version of the Rossby Centre regional atmospheric model—RCA4 (Samuelsson et al. 2011) is used in

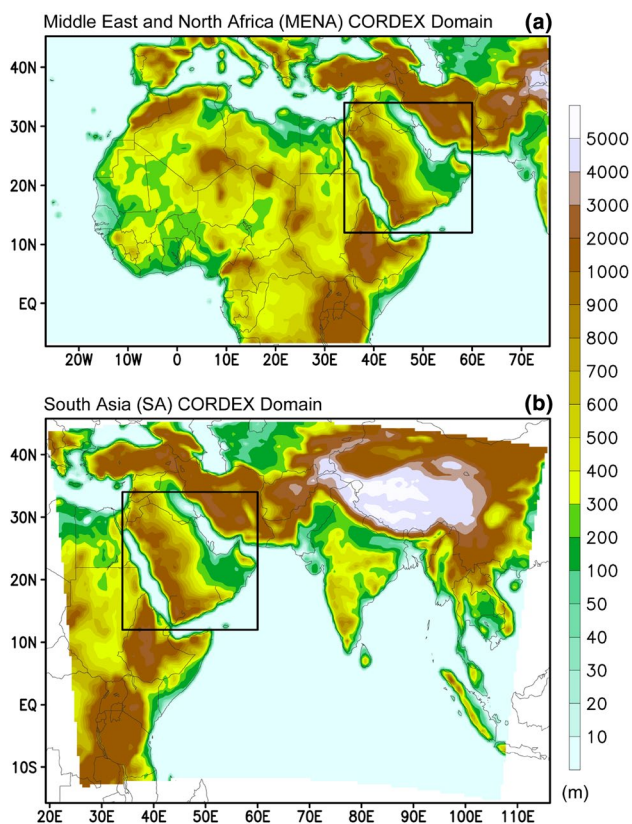


Fig. 1 Topographic map of Middle East and North Africa (a) and South Asia (b) RCA4 CORDEX simulations. Shading represents surface elevation in meters using RCA4 surface altitude data. Rectangular box shows the study region, indicating the common region over the two different simulation domains

Table 1 Observed precipitation and temperature datasets used in this study

S. no.	Dataset (precip)	Resolution	Period	References
1	CRU TS v. 4.01	0.5M	1901–2016	Harris et al. (2014)
2	CPC-Unified	0.5D	1979–2005	Xie et al. (2010)
3	GPCC V7	0.5M	1901–2013	Schneider et al. (2015)
4	UDEL v5.01	0.5M	1901–2017	Willmott and Matsuura (2001)
5	EWEMBI1	0.5D	1979–2016	Frieler et al. (2017)
S. no.	Data set (temp)	Resolution	Period	References
1	CRU TS v. 4.01	0.5M	1901–2016	Harris et al. (2014)
2	CPC	0.5D	1979–2018	Beck et al. (2017)
3	GHCN-CAMS	0.5M	1948–2018	Fan and Van den Dool (2008)
4	UDEL v5.01	0.5M	1901–2017	Willmott and Matsuura (2001)
5	EWEMBI1	0.5D	1979–2016	Frieler et al. (2017)

the MENA-CORDEX and SA-CORDEX to downscale the following CMIP5 GCMs: (1) EC-EARTH with horizontal resolutions are $1.125^\circ \times 1.125^\circ$ (2) Centre National de Recherches Météorologiques CNRM-CM5 at a resolution of $1.4^\circ \times 1.4^\circ$ (3) NOAA Geophysical fluid dynamics Laboratory GFDL-ESM2M with horizontal grid resolution of approximately 2° .

RCA4 has been set up and run for both CORDEX domains at horizontal resolution of 0.44° which corresponds to approximately 50 km grid spacing. Figure 1a, b show the RCA4 MENA-CORDEX and SA-CORDEX simulation domains, respectively with AP as the study area, which is a common region between two domains (shown as rectangular boxes). A first set of runs consists of downscaling of ERAINT reanalysis data. These simulations are used for evaluating model performance in the recent-past climate. In a second round, RCA4 has been used to downscale data of three different GCMs. The simulations have been performed for the, (1) historical period (1951–2005) for which historical forcing was applied and (2) different future (2006–2100) Representative Concentration Pathways (RCPs) scenarios (Moss et al. 2010) which have been applied to prescribe possible range of future radiative forcing values in the year 2100. Greenhouse gas concentrations are expressed as equivalent CO_2 concentrations following the RCP scenarios, and interpolated from 1 year to the next. In this study, we used the RCP 8.5 scenario which represents the category of ‘high GHG emission scenario’ and prescribes the future radiative forcing level approximately 8.5 W/m^2 by the end of twenty-first century.

2.3 Methodology

The model results of both MENA-CORDEX and SA-CORDEX domains for RCA4 simulations with ERAINT LBC are compared with the observed temperature and

precipitation by calculating simple biases and time series analysis of two distinct subdomains over the AP for the period 1981–2005. The details of selected subdomains are described in Sect. 3.1.2. The analysis was performed on seasonal (summer and winter) and annual time scales. The annual cycles of GCMs and RCA4 simulations (with ERAINT and different GCMs boundary condition) are calculated. Taylor diagram (Taylor 2001) is made for selected subdomains. A Taylor diagram can provide concise statistical calculations of how well the spatial patterns of different models and observations match each other in terms of correlation coefficient, the centered Root Mean Square Difference (RMSD), and the standard deviation for the seasons. The sensitivity of domain is examined by calculating the differences between two CORDEX domains for the base period (1976–2005) and also for the future period (2071–2100). The RCA4 simulation differences are also checked for different driving GCMs for assessing the sensitivity to the LBCs along with the domain differences. The projected changes during the period 2071–2100 with respect to the base period of 1976–2005 in the mean temperature and precipitation are calculated for the AP for both CORDEX domains and driving GCMs under RCP8.5 scenario. The Sen’s method (Sen 1968) is used to calculate the slope of the linear trends and Mann–Kendall test (Mann 1945; Kendall 1975; Gilbert 1987) is used to check the statistical significance (at 5% level) of trends in the temperature and precipitation time series.

The climate of AP can be classified into two broader seasons (Almazroui 2011), i.e., wet (November to April) and dry (May to October). The differences in the large-scale circulation patterns (MSLP, Winds (U and V) and Specific Humidity) are also studied in order to understand the physical basis for the differences between RCA4 temperature and precipitation simulations for both CORDEX domains and different driving GCMs.

3 Results and discussions

3.1 Model evaluation for MENA and SA CORDEX simulations

3.1.1 Climatology of temperature and precipitation and model biases

The observed mean (1981–2005) temperature (°C) for dry season is shown in Fig. 2a. The temperature ranges from less than 18 °C (over the Asir Mountains covering south-western parts of Kingdom of Saudi Arabia (KSA) and the western parts of Yemen) to above 33 °C (over the eastern province of KSA). Attada et al. (2018) studied the surface air temperature variability and its associated large-scale circulation patterns over the AP and showed

that the lowest temperatures over the south-west AP are related to its proximity to the cold Arabian Sea waters, in addition to the orographic effects. The temperature is also lower over the north-western parts of AP covering northern parts of Tabuk and Jouf regions of KSA. Whereas in the wet season, the mean temperature over the northern AP is observed below 18 °C and remains below 24 °C over the desert (Empty Quarter) in the eastern province of KSA (Fig. 2b). The higher and lower mean temperature distribution can also be seen on annual time scales (Fig. 2c). The biases in the mean temperature in the MENA/SA CORDEX simulations are similar during the dry season (Fig. 2d, g). There is a warm bias (above 3 °C) over the south-eastern parts and cold bias (above 2 °C) over the western parts of AP. A warm bias can also be seen over the northern parts of AP. However, in case of wet season the cold bias from 1 to 4 °C is observed over

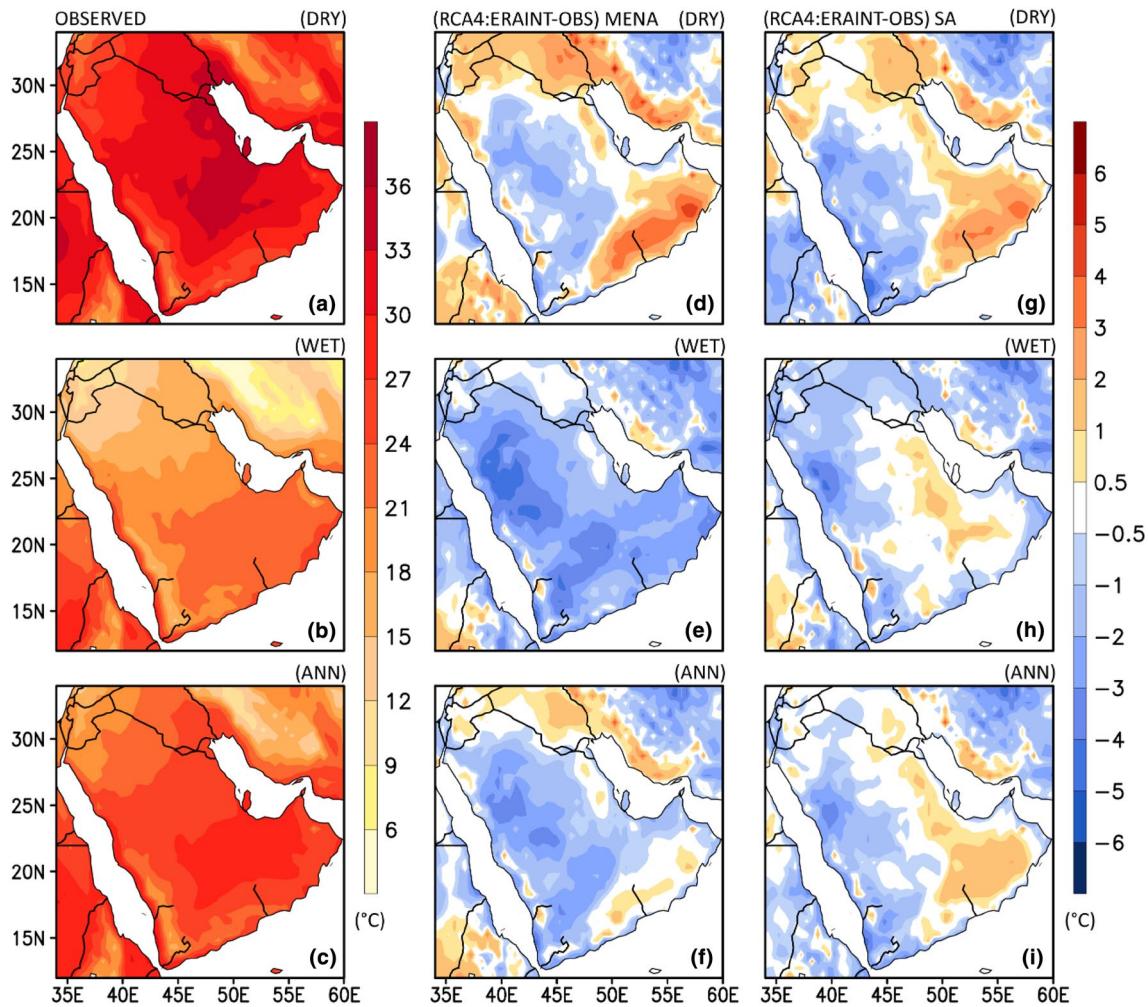


Fig. 2 a–c Observed mean temperature (°C) for dry (May–October), wet (November–April) and annual cases, respectively for the period 1981–2005. d–f Mean temperature (°C) bias of RCA4 (ERAINT) for

MENA simulations for dry, wet and annual cases, respectively. g–i Same as middle column (d–f), except for SA simulations

the whole AP in the MENA simulation (Fig. 2e), but this cold bias is restricted to only north-western parts of AP in case of SA simulation (Fig. 2h) and a warm bias is visible over the eastern province of KSA. This warm bias is more evident in the annual mean temperatures (Fig. 2i). It has to be noted that there is no observational network over the desert (Empty Quarter) in the eastern province of KSA. The RCA4 simulations with ERAINT for MENA are colder during the wet season compared to SA simulation, especially over eastern parts (desert areas) of AP.

The observed mean (1981–2005) annual precipitation (mm/month) is shown in Fig. 3c. The precipitation exceeding 20 mm/month is observed over Asir Mountains in the south-western parts of AP. The north-eastern parts of KSA also receive some precipitation, below 8 mm/month. Oman and United Arab Emirates (UAE) receive above 6 mm/month precipitation. The climate of the most parts of AP is hyper arid and remains dry throughout the year (Almazroui

et al. 2012). Most of the precipitation during dry season is received over the south-western parts of AP, particularly over the Asir Mountains (Fig. 3a), which is associated with the northward shifting of Inter Tropical Convergence Zone (ITCZ) apart from the topographically-driven convective events (Almazroui 1998; Abdullah and Al-Mazroui 1998). The details of spatial distribution of rainfall and its related large-scale mechanisms are described by Subyani (2004). During the summer season, most of the AP remains dry. In wet (winter) season, the northern parts of AP receive more than 14 mm/month mean precipitation associate with eastward moving westerlies and extension of Sudan low (Fig. 3b). There is a wet bias during the dry season in both MENA and SA simulations with more than 30 mm/month is noted over the Asir Mountains (Fig. 3d, g), whereas a dry bias is mainly observed over the whole AP in the wet season (Fig. 3e, h). This dry bias is more evident in the MENA simulation (Fig. 3e, h). This dry bias is more evident in the MENA simulation (Fig. 3e). The overall MENA domain simulation

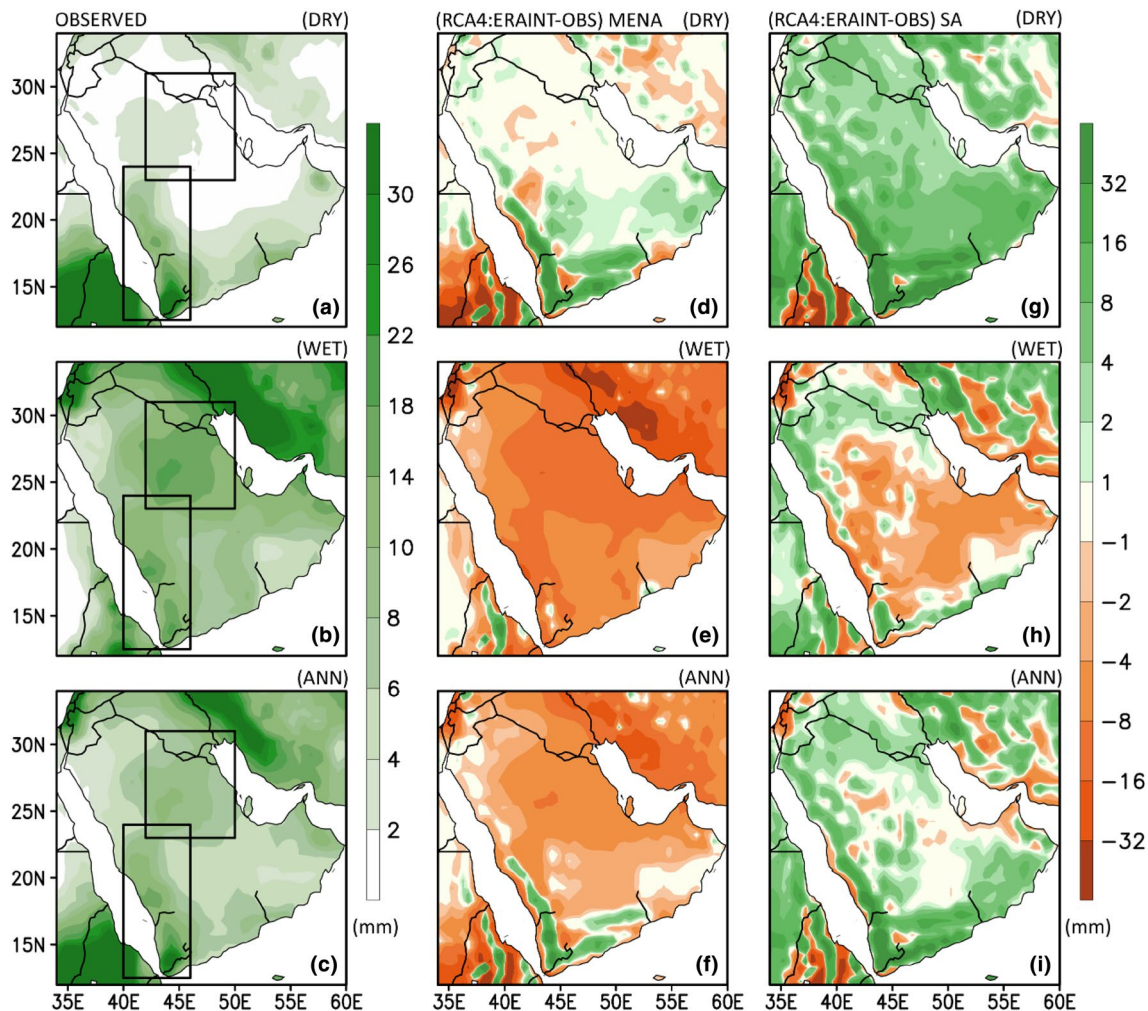


Fig. 3 As Fig. 2 but for the observed mean precipitation (mm/month). Upper and lower rectangles show North-East (NE), and South-west (SW) subdomains over the Arabian Peninsula, respectively

is drier compared to SA domain simulation, except over the Asir Mountains (Fig. 3f, i). It should again be noted that there is also an observational uncertainty over this region as there are very few meteorological stations located in this region, especially over the mountains.

3.1.2 Annual cycle and spatial evaluation of temperature and precipitation

There are clearly two distinct regions of precipitation shown as two rectangular boxes in Fig. 3a–c. In the winter season, the north-eastern parts (23–31°N, 42–50°E) of AP mainly receives precipitation from the interaction of westerlies (low pressure systems moving towards east from the Mediterranean Sea) and the Sudan trough (extension of Sudan Low) (Abdelmola 2009). Whereas in summer the south-western parts (12.5–24°N, 40–46°E) of AP receives precipitation influenced by the south Asian monsoon and Sudan low as a result of the northward shifting of ITCZ. The mean rainfall in the summer season is not influenced by the Mediterranean weather conditions (Abdelmola 2009). Based on these two main precipitation zones in winter and summer seasons, the north-east and south-west boxes (Fig. 3a–c) are selected to study the annual cycle of temperature and precipitation. The same subdomains are also used in the time series analysis of projected temperature and precipitation in the following Sect. 3.2.

The annual cycle of observed and simulated temperature and precipitation for north-east and south-west regions of AP for both MENA and SA simulations are shown in Fig. 4. The RCA4 (ERAINT) annual cycle of temperature in the north-east subdomain is well simulated and is in agreement with the observations, however the cold bias (about 3 °C) can be seen in the winter months (Fig. 4a) for MENA simulation. GCMs and RCA4 driven by different GCMs simulations are showing cold bias throughout the year. In the south-west subdomain (Fig. 4b), the annual cycle is not well captured by EC-EARTH GCM, especially during summer months. The cold bias in the RCA4 simulations over south-west subdomain is similar to that as observed for north-east subdomain for both MENA and SA simulations. It is again noted that RCA4 (ERAINT) MENA simulations have cold biases compared with SA simulations during winter months. Generally, SA simulations of temperature are closer to observations compared to MENA simulations. In case of precipitation (Fig. 4c, d), the RCA4 (ERAINT) annual cycle is better simulated by SA simulation compared to MENA simulation. MENA simulation is underestimating the precipitation, especially in winter (more than 10 mm/month) in the north-east subdomain (Fig. 4c). In the south-west subdomain, the precipitation simulated by the EC-EARTH GCM is going above 150 mm/month during summer (secondary axis in Fig. 4d). The double peak in precipitation annual cycle in

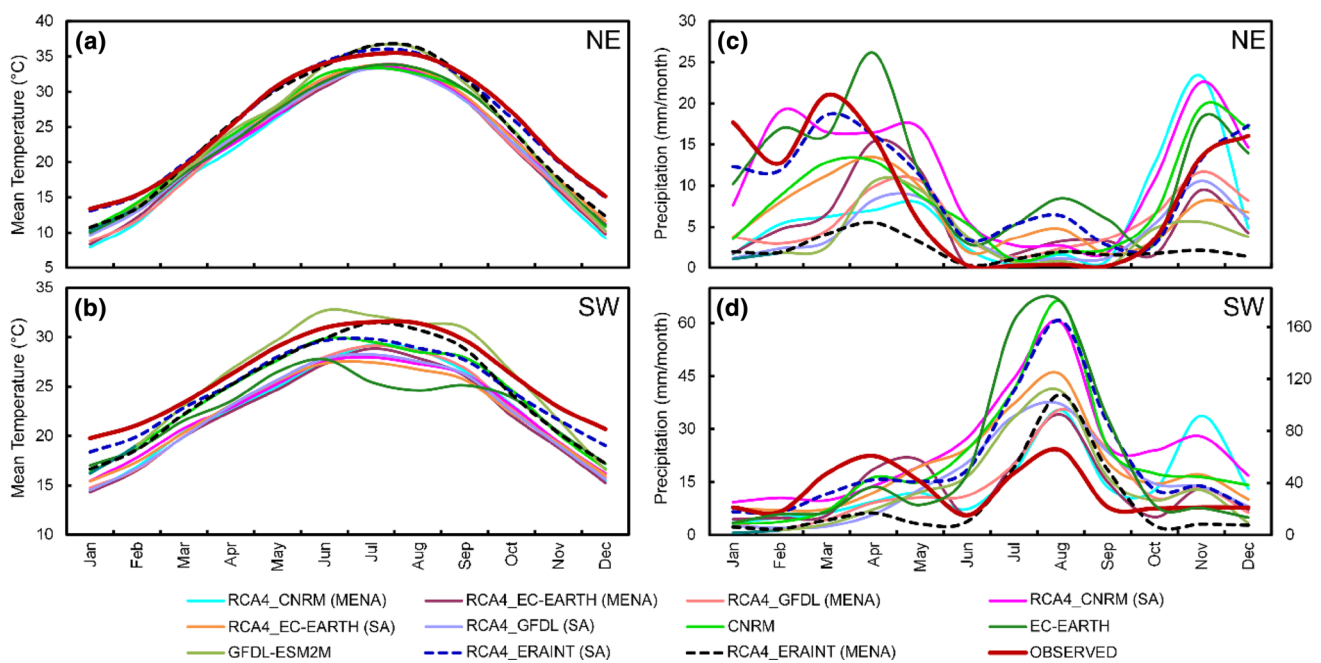


Fig. 4 a, b Annual cycle of observed, GCMs, and RCA4 simulated past (1981–2005) mean surface temperature (°C) for North-East (NE) and South-West (SW) subdomains, respectively for MENA and SA simulations with ERAINT, CNRM-CM5, EC-EARTH, and GFDL-

ESM2M lateral boundary conditions. c, d Same as a and b except for mean precipitation (mm/month) for NE and SW subdomains, respectively. In d, the secondary vertical axis on the right side is for EC-EARTH GCM, as the value approaches 160 mm/month

the observations during spring and summer is captured by both MENA and SA simulations; however, both simulations underestimate the strength of annual cycle in the spring season. It can also be noted that the MENA/SA simulations produce a wet bias in the summer months, especially in the month of August. The monthly mean and standard error for multi-observed mean near surface air temperature ($^{\circ}\text{C}$) and precipitation (mm/month) over the North-East and South-West Arabian Peninsula are given in Table 2. The small values of standard errors for both temperature and precipitation show that the differences among five observational datasets are not large.

The statistical analysis of the spatial patterns of mean (1981–2005) temperature and precipitation over the whole AP (analysis domain, Fig. 1) of different GCMs and RCA4 (driven by ERAINT and GCM outputs) in the MENA/SA simulations is presented in the Taylor diagram (Fig. 5). Statistics for RCA4 model, driven by ERAINT and different GCMs, are computed to quantify how closely models' simulation pattern matches with a reference field. The spatial correlations of RCA4 simulations of temperature lie between 0.9 and 0.95 for both dry and wet seasons, respectively, whereas GCMs have large differences especially in dry season. The RMSD is less in the wet season compared to dry season, whereas the standard deviation well approximates the observations. Overall, the RCA4 for both simulation domains has relatively high spatial correlation with low RMSD for both seasons. It is also noted that the MENA and SA temperature simulations are clustering separately during the dry season, this clustering is also visible in case of precipitation during dry season. The spatial correlations of simulated precipitation are above 0.8 for both the seasons and simulations, whereas the standard deviation is not well captured during the wet season. EC-EARTH GCM shows a

very high standard deviation and RMSD, especially in the dry season (Fig. 5).

3.1.3 Differences between two CORDEX simulation domains

The sensitivity of regional climate model to MENA/SA simulation domains and different LBCs is discussed in this section. The results in Fig. 6 are presented as the differences between MENA and SA simulations for seasonal (dry and wet) and annual temperatures with ERAINT and GCM-driven boundary conditions. In case of dry season (Fig. 6, left column); the model (driven by ERAINT and GCM outputs) simulates the highest (above 2°C) temperatures over most of the AP and lowest (around 2°C) in the central parts of KSA for MENA compared to SA simulation. This spatial pattern remains similar irrespective of different LBCs. Similarly, for the temperature differences between MENA and SA simulations during wet season, the MENA temperature simulations are lower over almost the whole AP with a minor effect of different LBCs (Fig. 6, middle column). However, MENA simulations are warmer (between 1° and 2°) over the eastern Africa and north-western AP. The results for annual case are similar to those found in the wet season (Fig. 6, right column). It can also be noted that the magnitude of the differences between MENA and SA simulations for RCA4 driven by GFDL-ESM2M is slightly lower compared to ERAINT and other GCMs-driven model, showing some effects of LBCs.

In the case of a precipitation (Fig. 7), RCA4 (ERAINT) MENA simulations are drier in both the seasons compared to SA simulations (Fig. 7, top row). RCA4 with LBCs of CNRM-CM5 GCM also show similar dry pattern (Fig. 7, second row), with the exception over the desert (Empty

Table 2 Standard Error (SE) for multi-observed mean near surface air temperature ($^{\circ}\text{C}$) and precipitation (mm/month) over the North-East and South-West Arabian Peninsula

Month	North-East (NE)				South-West (SW)			
	Temperature		Precipitation		Temperature		Precipitation	
	Mean	SE	Mean	SE	Mean	SE	Mean	SE
JAN	13.41	0.28	17.71	0.15	19.78	2.01	7.83	1.09
FEB	15.36	0.27	12.73	0.21	21.09	1.81	6.58	1.39
MAR	19.46	0.25	21.02	0.13	23.38	2.48	17.38	2.18
APR	25.17	0.23	15.99	0.18	26.21	2.22	22.41	2.31
MAY	30.91	0.18	5.39	0.14	29.05	1.11	15.09	1.80
JUN	34.01	0.16	0.29	0.12	30.95	0.06	5.62	0.83
JUL	35.32	0.17	0.25	0.12	31.52	0.06	17.51	1.47
AUG	35.20	0.22	0.40	0.11	31.41	0.08	24.01	1.93
SEP	32.35	0.14	0.23	0.11	29.69	0.05	7.94	0.59
OCT	27.14	0.19	3.51	0.12	26.22	0.81	7.54	1.62
NOV	20.29	0.19	13.55	0.12	22.92	2.77	7.84	1.45
DEC	15.18	0.30	16.09	0.13	20.70	2.36	7.79	1.07

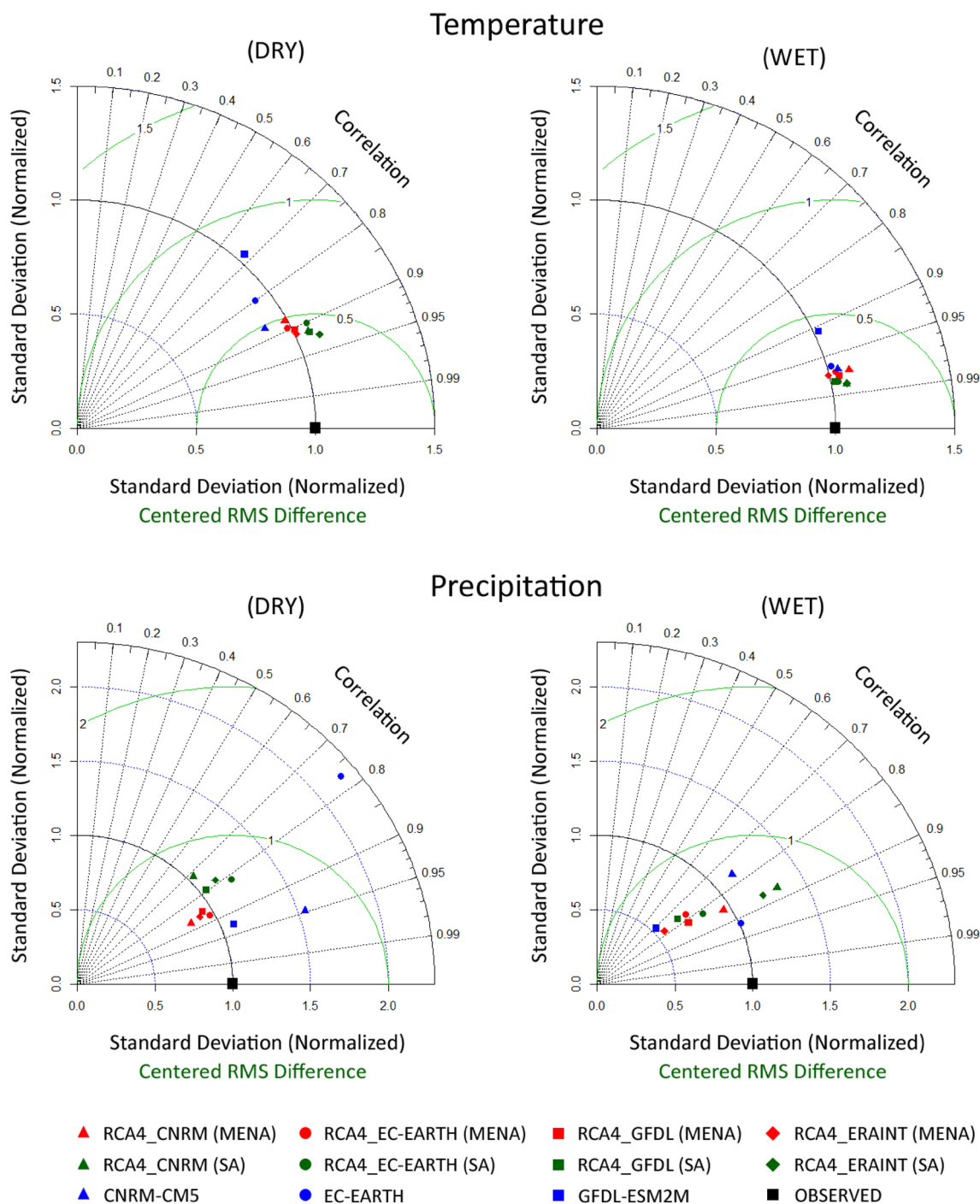


Fig. 5 Top row: Taylor diagram showing a statistical comparison of spatial patterns with observation of three different GCMs and RCA4 simulated past (1981–2005) annual mean surface temperature (°C) for AP, for MENA and SA simulations with ERAINT, CNRM-CM5,

EC-EARTH, and GFDL-ESM2M lateral boundary conditions. Bottom row: same as top row except for annual mean precipitation (mm/month)

Quarter) areas of KSA during wet season. The magnitude of this difference in the precipitation due to difference in the simulation domain (MENA/SA) is comparable to the mean precipitation (Fig. 3, left column) observed over the region. However, in case of RCA4 (EC-EARTH) and

RCA4 (GFDL-EM2M), the eastern parts of AP are wet in MENA simulations compared to SA simulations (Fig. 7, bottom rows). It should be noted that the simulation of temperature seems to be very sensitive to the simulation domain (MENA/SA) and not sensitive to different LBCs,

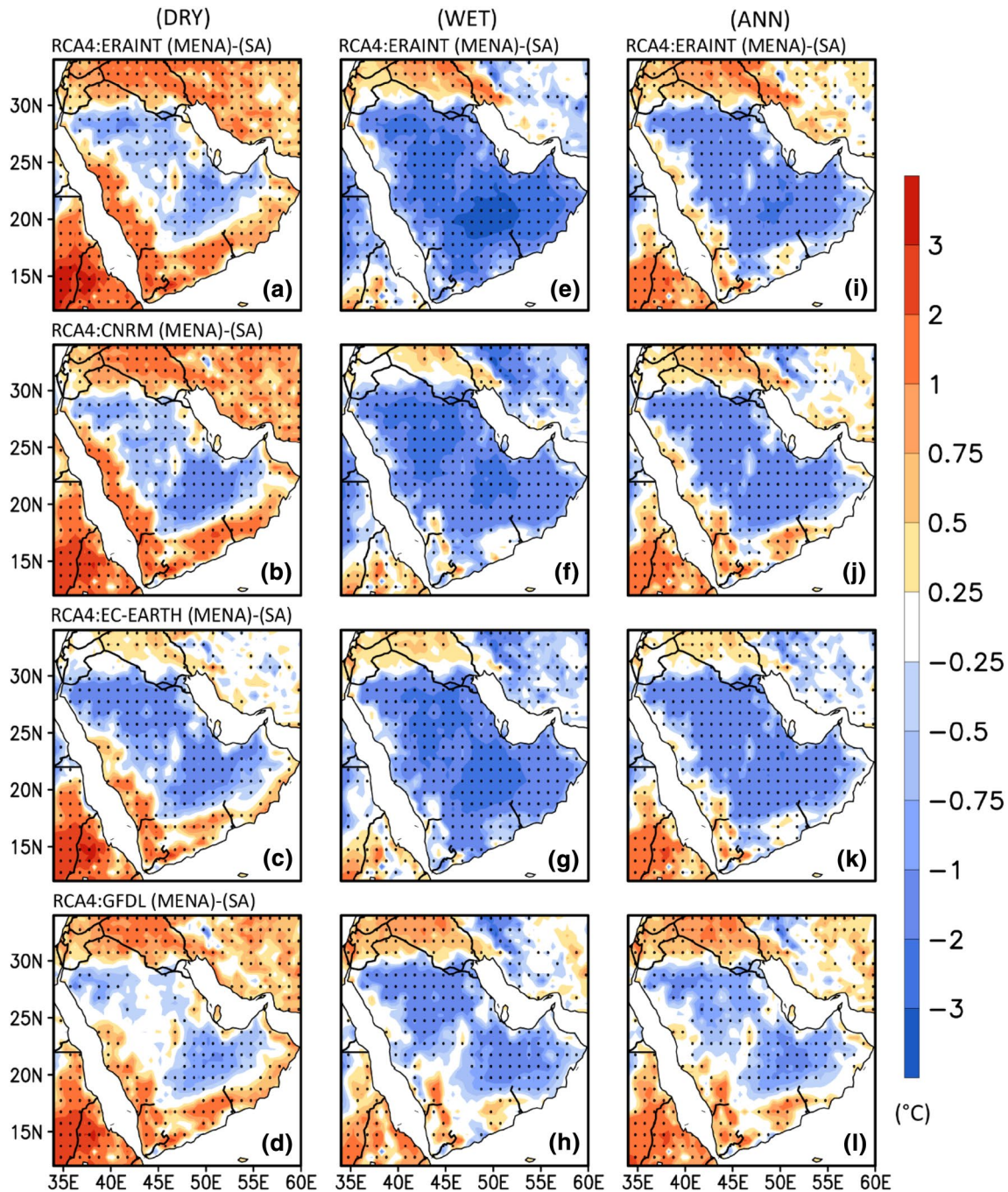


Fig. 6 a–d The difference between RCA4 simulated past (1981–2005) mean surface temperature (°C) with ERAINT, CNRM-CM5, EC-EARTH, and GFDL-ESM2M, respectively lateral boundary con-

ditions for MENA and SA simulations during dry season. e–h and i–l Same as left column (a–d) except for the wet and annual case, respectively. Black dots show significance at 95% level

whereas in case of precipitation LBCs seem to play dominant role.

3.1.4 Differences in large-scale circulation and humidity

We have also emphasized investigating the differences in large-scale circulation between MENA and SA simulations

over the selected common domain (i.e., AP and its surrounding areas) in order to see if the differences in the temperature and precipitation can be explained. The mean SLP and winds at 850 hPa for dry and wet seasons are shown in Fig. 8a, b, respectively. In dry season the southern regions of AP and northwestern parts of Arabian Sea are dominated with the south Asian summer

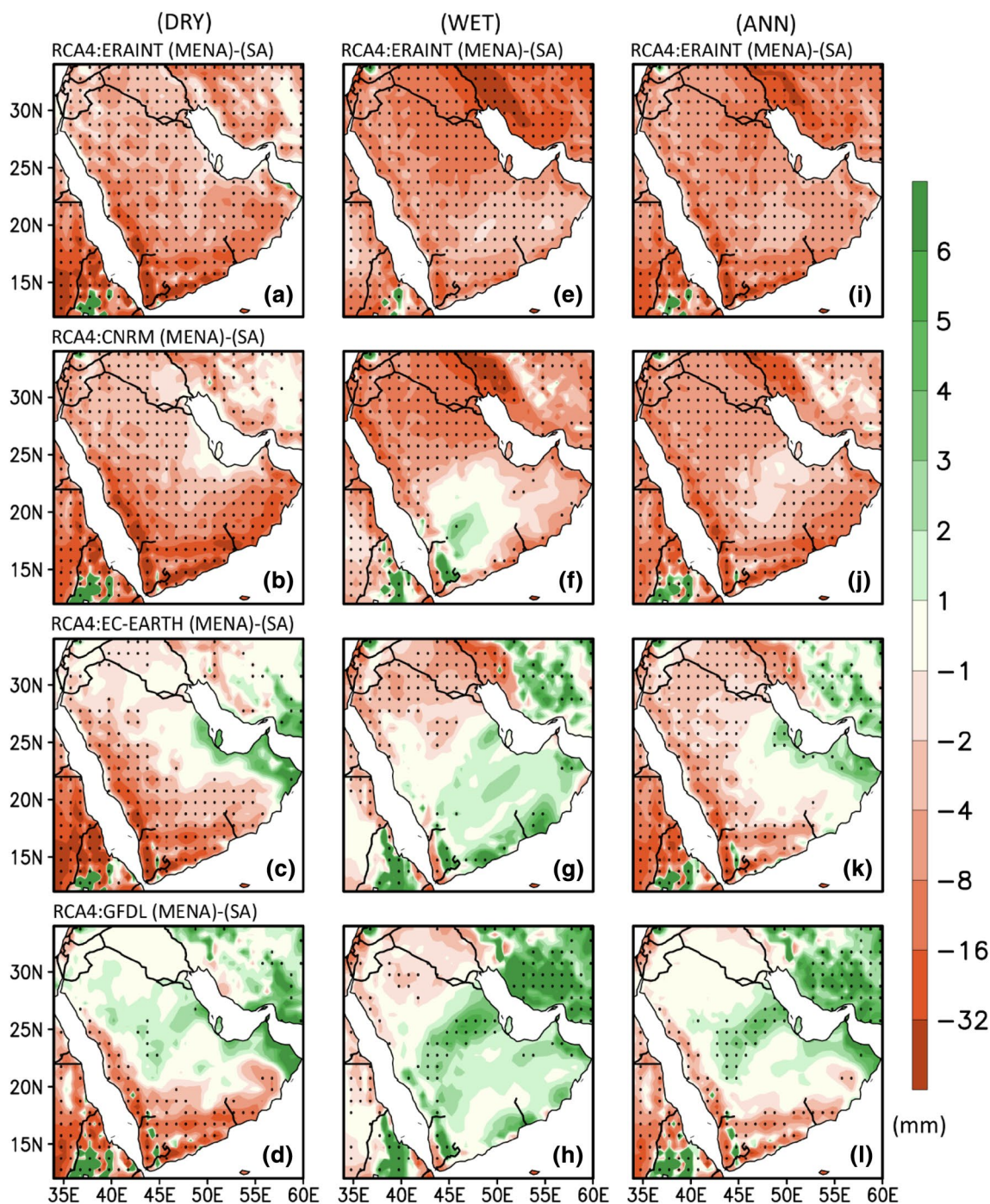


Fig. 7 As Fig. 6 but for the mean precipitation (mm/month)

monsoon circulations. This cyclonic flow pattern during the monsoon season contributes mainly to the wet conditions over the south-west subdomain (particularly over the highlands of Yeen), southern Oman and UAE. The heat low, which develops during May–September over Pakistan and north-west India (Bollasina and Nigam 2011), with its elongated westward extension towards AP can also be

seen in the Fig. 8a. The position of the ITCZ can also be identified from the convergence of winds from north and south between 10°N and 20°N from west to eastern parts of the domain. A ridge of high pressure can be seen in the MSLP and winds (anti-cyclonic) over AP in the wet season (Fig. 8b). The difference between MENA and SA simulation of RCA4 (ERAINT) during dry season show

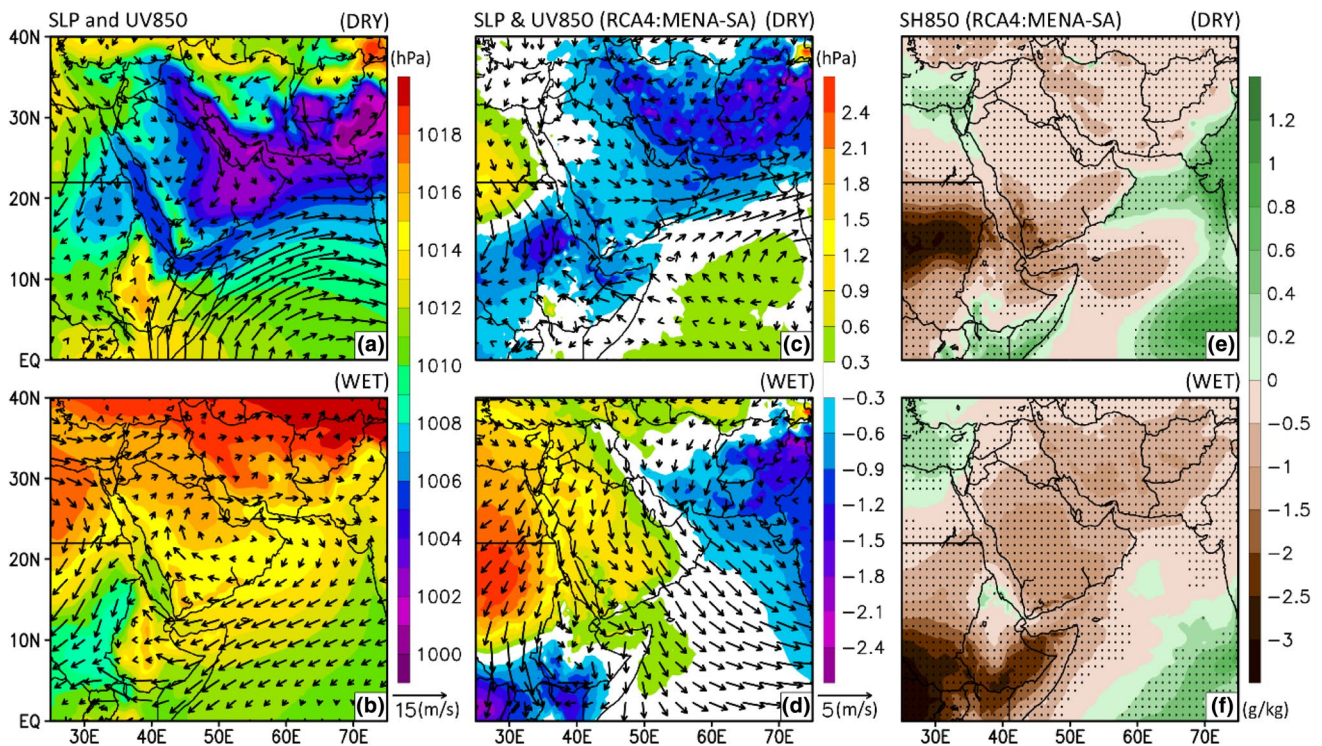


Fig. 8 **a, b** Observed (ERAINT) climatology of mean sea level pressure (shaded, hPa) and 850-hPa winds (arrows, m/s) for dry and wet seasons, respectively. **c, d** Same as **a, b** except for the difference between RCA4 MENA and SA simulations (1981–2005) with

ERANT lateral boundary conditions. **e, f**: Same as **c, d** except for 850 hPa specific humidity (g/kg). Black dots show significance at 95% level

strengthening of monsoon flow over the northern parts of Arabian Sea and the southward flow from Sahara desert in the western parts of the domain (Fig. 8c). This intensified southward flow from the African desert region may be linked to the higher temperatures in the MENA simulations (Fig. 6a), whereas the stronger monsoon flow is advecting moisture eastward from AP, resulting in higher specific humidity in the eastern parts of the domain and lower specific humidity over the western parts including AP (Fig. 8e). The decreased humidity over the AP in the MENA simulation compared to SA simulation maybe attributed to decreased precipitation over AP (Fig. 7a). During wet season, the northerly flow strengthens over most parts of the domain (Fig. 8d). This intensified southward flow from the AP and its adjoining areas may likely be linked to the lower temperatures in the MENA simulations over the region (Fig. 6e). It is again noted that, the higher specific humidity conditions in the south-eastern parts of the domain (east Arabian Sea) and lower over the AP and its western parts may be associated with the strong southward advecting moisture flow from the north (Fig. 8f). A lower specific humidity over the AP in the MENA simulation compared to SA simulation during wet season is a likely reason for the decreased precipitation over the AP (Fig. 7e).

3.2 Projected changes in future mean temperature and precipitation for two CORDEX simulations

Climate change scenarios of mean temperature and precipitation have been developed for the year 2100 for RCP8.5 emission scenario. Radiative forcing reaches 8.5 W/m^2 by the end of this century. Figure 9 shows mean temperature climate change scenario of the dry season for 2100 (2071–2100), with respect to the historical model simulations for the period 1976–2005 for GCMs (CNRM-CM5, EC-EARTH and GFDL-ESM2M) and RCA4 with LBCs of these GCMs, for both MENA and SA simulations. CNRM-CM5 GCM is showing warming over the AP up to $4.8 \text{ }^\circ\text{C}$ (Fig. 9a), whereas in case of EC-EARTH and GFDL-ESM2M the warming is going up to $5.7 \text{ }^\circ\text{C}$ (Fig. 9e, i). This difference in the warming by different GCMs is also visible after downscaling by RCA4 for both MENA and SA simulations (Fig. 9, second and third row). It is also noted that EC-EARTH and GFDL-ESM2M GCMs show a bit more warming, especially over the north AP, compared to CNRM for both MENA and SA simulations. The warming (up to $4.8 \text{ }^\circ\text{C}$) projected by RCA4 with CNRM boundary conditions is mainly confined to the areas above 25°N latitude in the SA simulations (Fig. 9c). The differences between RCA4 MENA and SA simulations

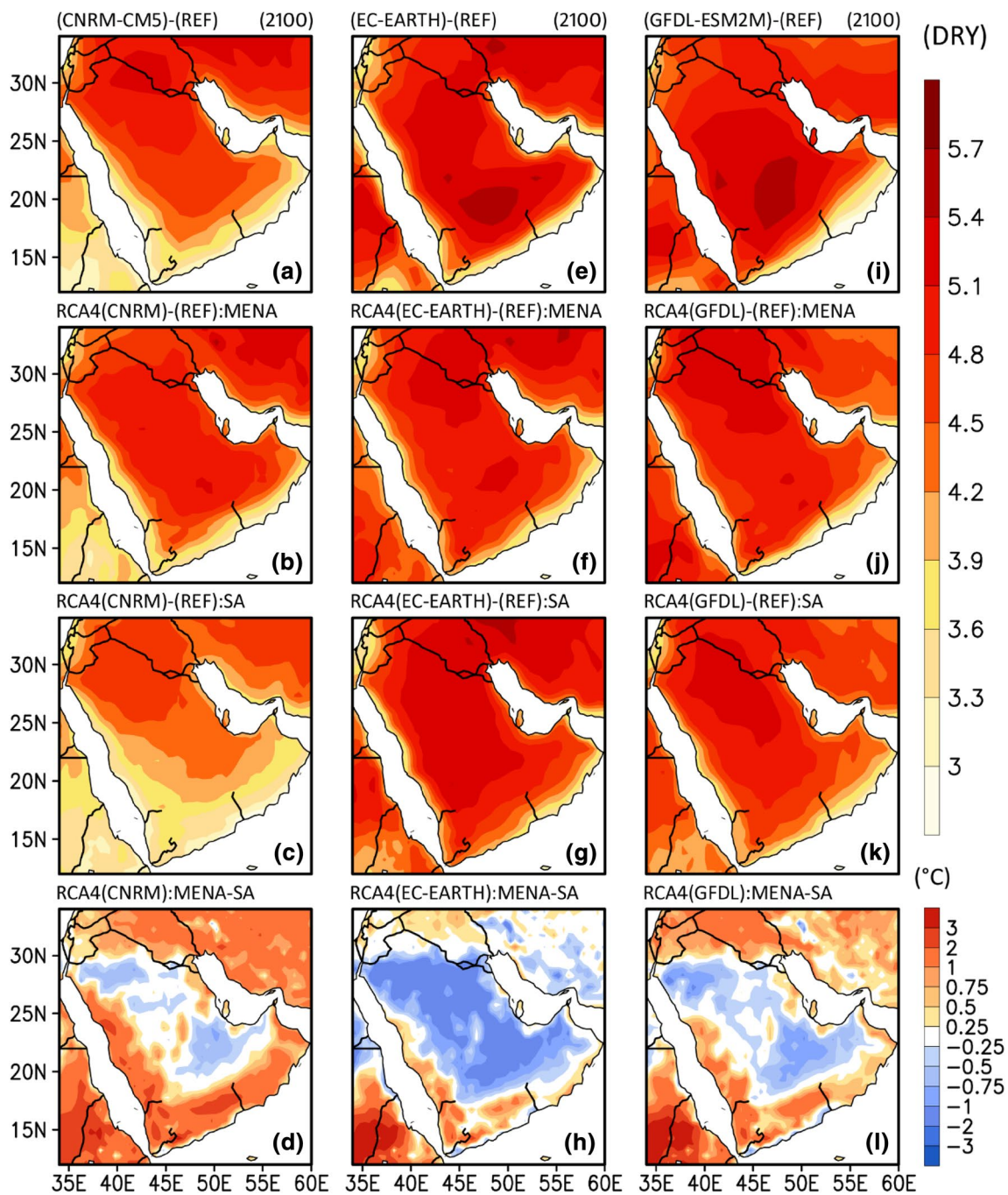


Fig. 9 a–c Changes in projected (2071–2100) mean temperature ($^{\circ}\text{C}$) with respect to recent past (1976–2005) during dry season, obtained from CNRM-CM5 and RCA4 simulations with CNRM-CM5 lateral boundary conditions for MENA and SA simulations, respectively under RCP 8.5 scenario. The bottom figure (d) shows the same as

above, except for the projected difference between MENA and SA simulations. Middle and Right columns: Same as left column except for RCA4 simulations with EC-EARTH and GFDL-ESM2M lateral boundary conditions

projected warming for different LBCs (Fig. 9, bottom row) show strikingly similar patterns as for the differences in the downscaled historical simulations (Fig. 6b–d). Similarly, during wet season the differences between the projected warming (Fig. 10, bottom row) is similar to that

as observed for the differences in the downscaled historical simulations (Fig. 6f–h). In the MENA simulations, the warming signal is about 2°C less compared to SA simulations over the whole AP (Fig. 10, bottom row). The warming by the end of twenty-first century in the wet

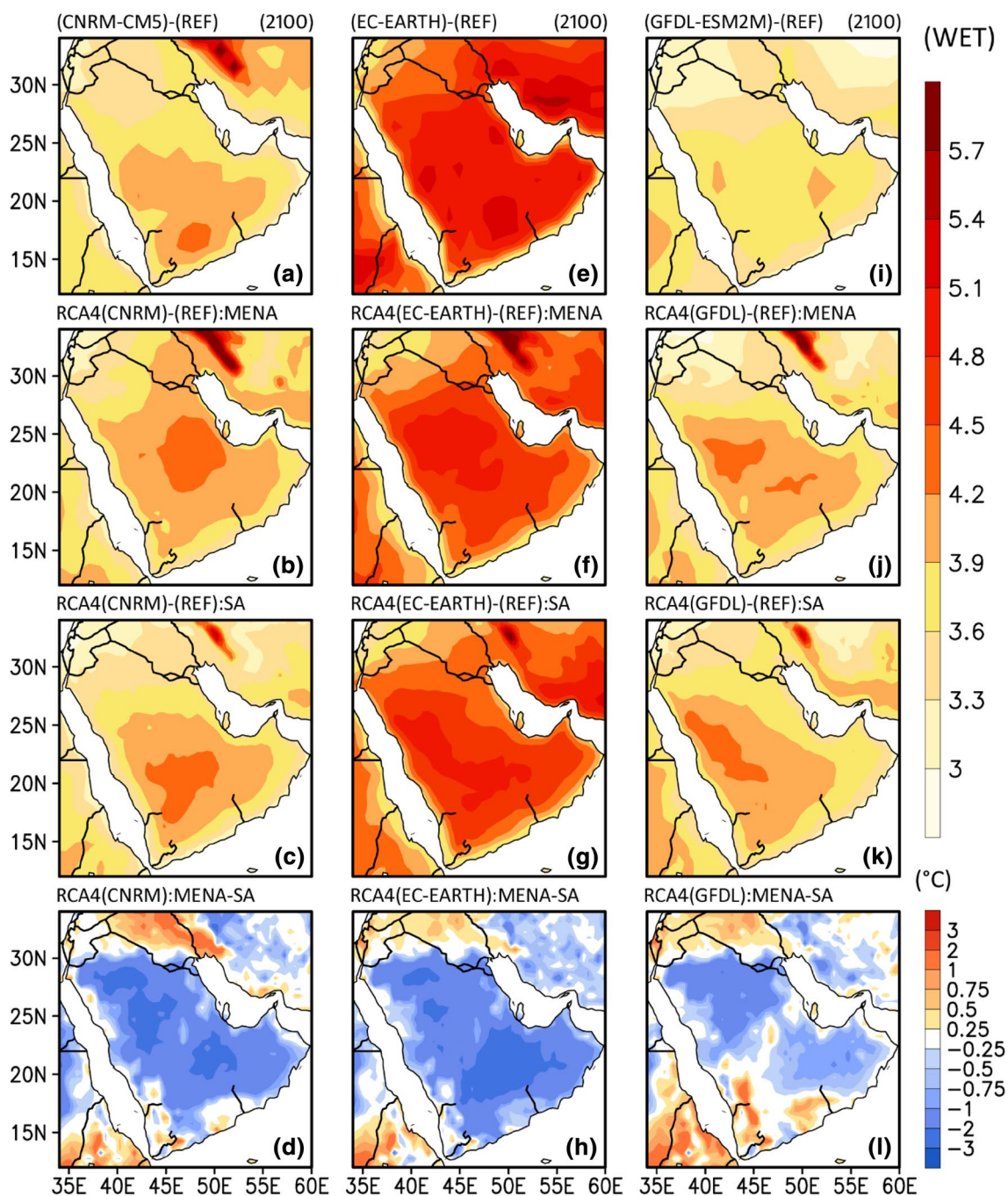


Fig. 10 As Fig. 9 but for the wet season

season is generally less compared to dry season, except for EC-EARTH GCM. The increase in mean temperature is around 4.2 °C in case of CNRM-CM5 and GFDL-ESM2M GCMs, as well as in the downscaled GCMs. The difference in the simulation domain (i.e., MENA and SA) is resulting in a difference of about 2 °C in the warming by the end of this century, showing that not only the historical simulations are affected by the choice of simulation domain but the projected changes in the temperature under RCP

scenarios are also very sensitive to the domain selection, which is comparable to the differences arising due to different LBCs.

In case of precipitation, the GCMs are projecting mixed climate change signal by the end of twenty-first century (Fig. 11, top row) during dry season. CNRM-CM5 shows slightly more (about 8 mm/month) precipitation in the future simulations, whereas EC-EARTH and GFDL-ESM2M simulate decreased precipitation over the AP.

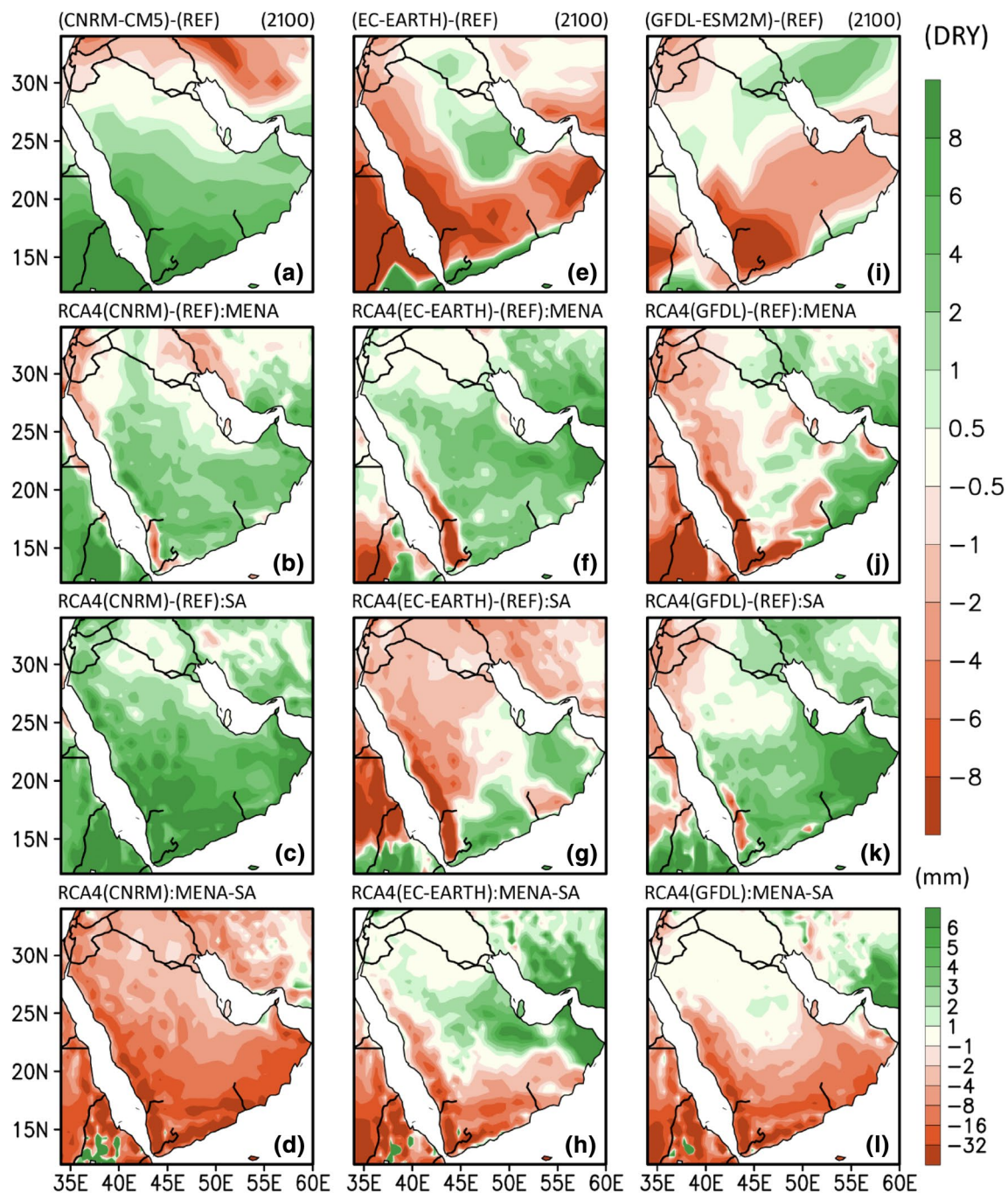


Fig. 11 As Fig. 9 but for the mean precipitation (mm/month)

The projected changes in the precipitation are slightly modified after downscaling with RCA4 in MENA and SA simulations (Fig. 11, middle rows). There is an increase in precipitation over the AP, except over the Asir Mountains, in the MENA simulations with RCA4 (CNRM-CM5 and EC-EARTH; Fig. 11b, f), while a decrease in precipitation (except over the eastern AP) is noted in case of RCA4 (GFDL-ESM2M; Fig. 11j). The SA simulations

show increase in precipitation with RCA4 (CNRM-CM5 and GFDL-ESM2M; Fig. 11c, k), whereas a decrease is observed in case of EC-EARTH-driven RCA4 model (Fig. 11g). The difference between MENA and SA simulated precipitation for the period 2071–2100 is shown in Fig. 11 (bottom row). In general, MENA simulation is projecting drier climate compared to SA simulation and this difference due to simulation domain is comparable to

the projected climate change. Although there is a mixed projected precipitation signal for different LBCs and simulation domains, however the difference due to simulation domains in future is again strikingly similar to the differences observed in the historical simulations (Fig. 7b–d). During wet season, a decrease in precipitation is generally observed over the whole AP by the end of twenty-first

century, as projected by GCMs (Fig. 12, top row). After downscaling with RCA4, the signal remains same for MENA simulation but becomes slightly opposite in the SA simulation (Fig. 12, middle rows). In case of RCA4 (CNRM-CM5), the MENA simulation is drier compared to SA simulation, however the difference is not prominent in case of RCA4 driven by the LBCs of EC-EARTH and GFDL-ESM2M (Fig. 12, bottom row).

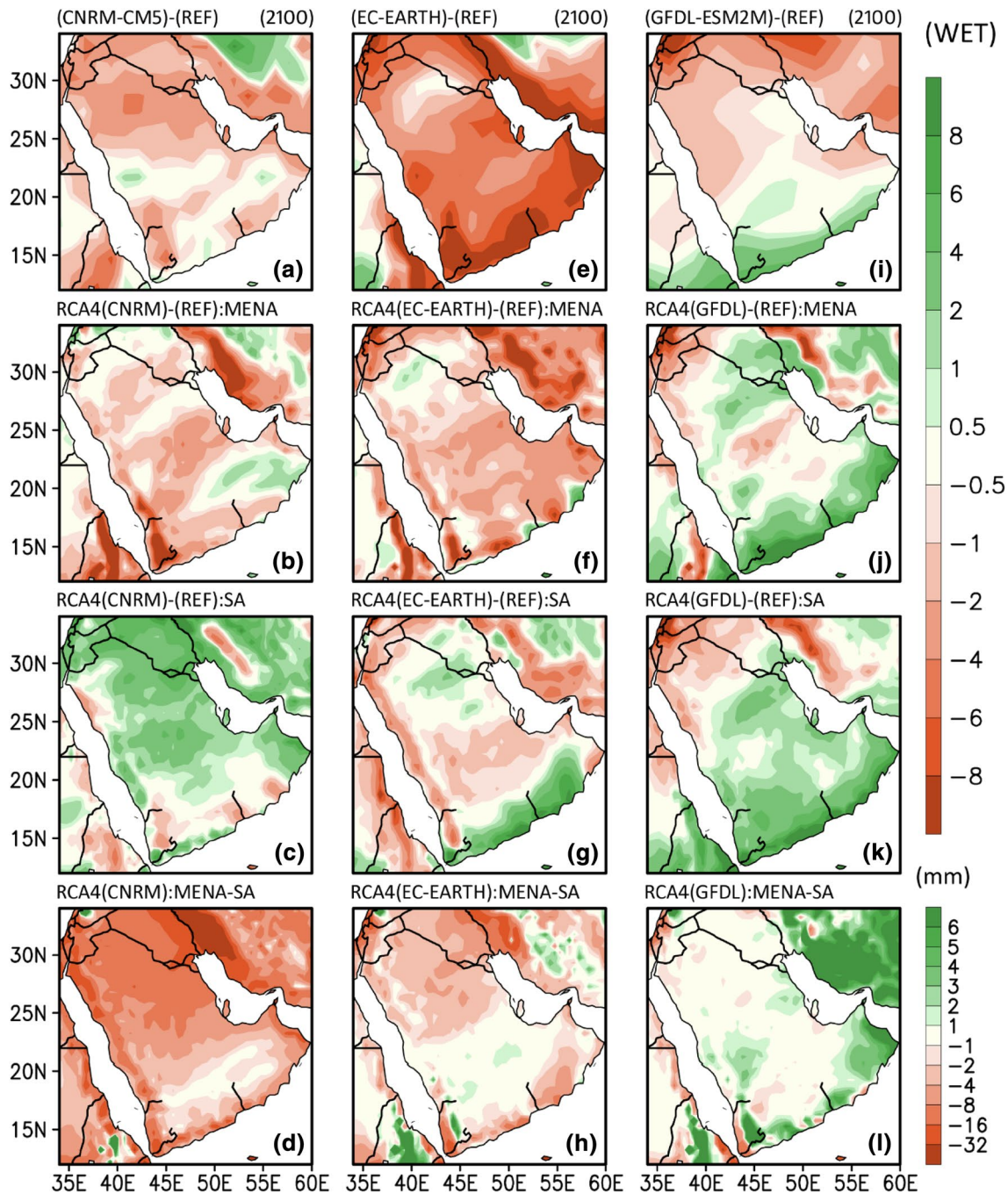


Fig. 12 As Fig. 11 but for the wet season

3.2.1 Time series analysis

As discussed in Sect. 3.1.2, two major regions were identified on the basis of different precipitation regimes in winter (wet) and summer (dry) seasons. The area average mean temperature time series of observed, historical and the future projections under RCP8.5 scenario over the north-east and south-west regions (subdomains) of AP are shown in Fig. 13. Both the observed and ensemble mean historical simulations are showing increasing trend in the past decades (1981–2005) with an increase in temperature from 0.6 to 1.0 °C. The slope of the observed temperature time series for both the subdomains is above 0.06 °C/year. The trend in the historical simulations of GCMs and downscaled GCMs with RCA4 are also showing statistically significant increasing trends during the period 1981–2005 (Fig. 13a, b). Both GCMs and RCA4 simulations are showing cold bias (about 2–3 °C); the cold bias is more in the downscaled simulations. In the north-east subdomain, the MENA simulation is clearly colder (above 1 °C) compared to SA simulation, whereas there is not much difference in case of south-west subdomain. This difference in temperature between MENA/SA simulations remains consistent up to the end of

twenty-first century (Fig. 13a). It should be noted that the south-west subdomain is dominated with precipitation in the summer related to ITCZ, whereas the north-east subdomain receives precipitation during winter season associated with eastward moving westerlies and Sudan trough. The difference in temperature among different GCMs is larger (about 2–3 °C), but after downscaling this difference is reduced in both historical and future simulations for both subdomains. This convergence behavior is typical for RCMs (Syed et al. 2014).

In case of precipitation, there is no significant trend in the past as well as in the future for both GCMs and RCA4 simulations over both subdomains (Fig. 13c, d). However, the precipitation over south-west (north-east) AP, i.e., over Asir Mountains subdomain is showing slightly decreasing (increasing) trend by the end of twenty-first century. RCA4 MENA simulations are drier (above 5 mm/month) compared to SA simulations, especially in the south-west subdomain for the whole period 1981–2100 (Fig. 13d). In the north-east subdomain, there is a clear difference in temperature for MENA and SA simulations but almost no difference is observed in the precipitation time series (Fig. 13a, c), and the situation is vice versa in south-west subdomain.

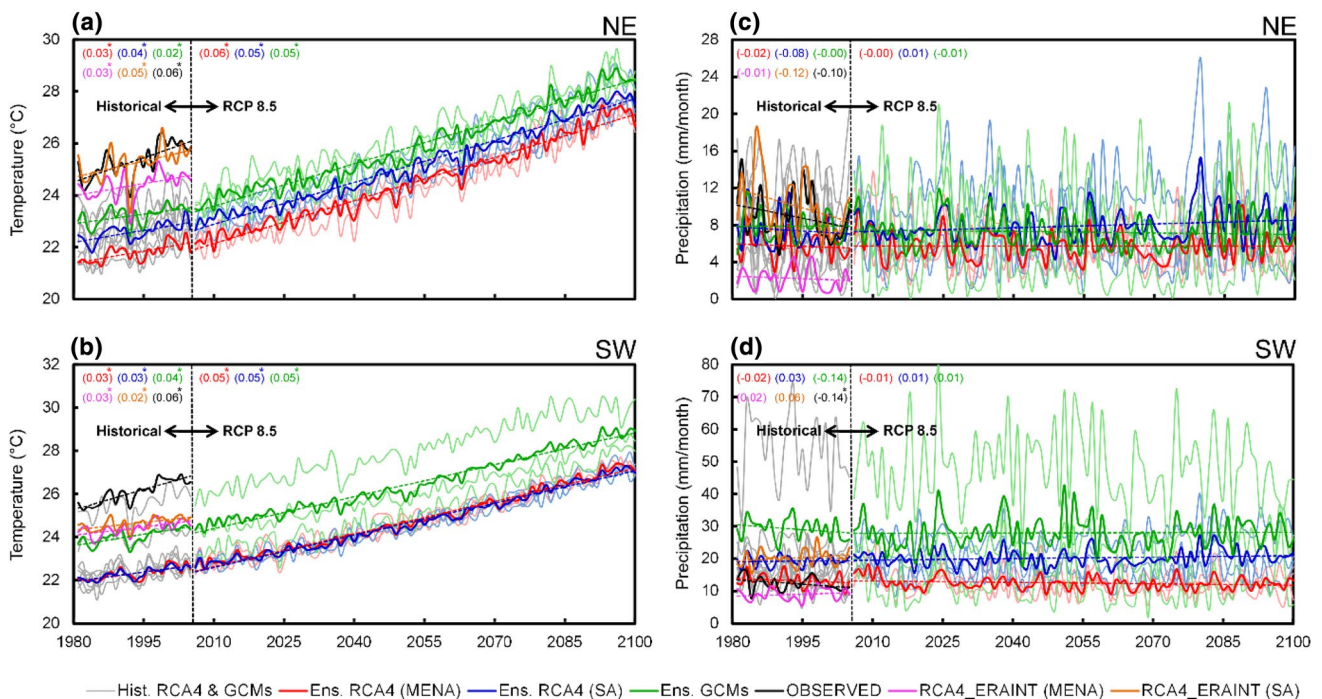


Fig. 13 a, b Mean annual temperature (°C) time series, area average over the North-East (NE) and South-West (SW) subdomains, respectively of Arabian Peninsula for MENA and SA simulations for historical (1981–2005) and future (2006–2100) periods under RCP 8.5 scenario. The brown lines represent multi-observed mean and the green, red, and blue thick lines show multi-model mean for GCMs, RCA4 (MENA), and RCA4 (SA) simulations, respectively. The dashed lines

show the linear trends in the time series. c, d Same as a, b except for annual precipitation (mm/month) for NE and SW subdomains, respectively. The values in parenthesis show slope of trend line (mm/month/year) using Sen's slope estimator. The trend in time series is checked at 5% significance level using MK test and is marked with asterisk

The difference in the temperature cannot be explained by the differences in the precipitation in the MENA and SA simulations. Therefore, some other dynamical or physical processes are responsible for these differences, which bear further investigation.

4 Summary and conclusions

In the COordinated Regional climate Downscaling EXperiment (CORDEX), a matrix of several RCM simulations (with LBCs of ERA-Interim reanalysis and different GCMs) is available for many regions (domains) of the globe, for historical (1951–2005) and future (2006–2100) periods under different RCP scenarios. Rossby centre RCM RCA4 has downscaled three GCMs, i.e., CNRM-CM5, EC-EARTH and GFDL-ESM2M for both MENA and SA CORDEX simulation domains, Arabian Peninsula (AP) is covered in both MENA and SA simulations. The differences between MENA and SA simulations for different LBCs in the historical (1976–2005) and future (2071–2100) time periods under RCP8.5 scenario is examined to study the effects of CORDEX domain and driving GCMs on the simulation of temperature and precipitation over the AP. The analysis is done for both winter (wet) and summer (dry) seasons. RCA4 simulations are capturing the observed temperature and precipitation patterns with some local biases. A wet bias of about 30 mm/month during summer season is observed over south-western parts of AP (Asir Mountains), whereas in winter season dry bias is present over the whole region. There is a cold bias (about 2 °C) over the north-western parts of Kingdom of Saudi Arabia, covering Madinah and Hail regions in both MENA and SA simulations and warm bias over eastern parts of AP during summer, whereas a cold bias (0.5–3 °C) is observed over the whole region, especially in case of MENA simulations during winter. The annual cycle of temperature and precipitation is well captured with cold bias throughout the year in GCMs and RCA4 driven by GCMs simulations. Generally, the annual cycle of SA simulations of temperature and precipitation are closer to observations compared to MENA simulations. Generally there are less biases in the temperature in the SA simulations compared to MENA simulations in both the seasons, however in case of precipitation there are less biases in the MENA simulations in dry season. The SA simulations are performing well in reproducing present climate of AP.

In case of dry season, higher temperatures over most of the AP with exception over the central parts of KSA are simulated for MENA compared to SA simulation. However during wet season, the MENA temperature simulations are lower over the whole AP. These lower temperatures in the MENA simulations compared to SA simulations maybe linked to intensified southward flow from the northern parts

of the domain. Different LBCs have little effect on these spatial patterns. The simulation of temperature seems to be very sensitive to the simulation domain (MENA/SA) and less sensitive to different LBCs. MENA simulations are drier in both the seasons compared to SA simulations in case of ERAINT boundary conditions, which may be attributed to lower specific humidity over the AP in the MENA simulation compared to SA simulation, but the eastern parts of AP are wet in MENA simulations of RCA4 with EC-EARTH and GFDL-ESM2M boundary conditions. In case of precipitation LBCs seems to play dominant role.

The differences in the MENA and SA simulations as seen in the historical simulations are also propagating in future, resulting in a difference of ~2 °C in the warming by the end of the century, which is comparable to the differences arising due to different LBCs and climate change. MENA simulation is generally projecting drier climate compared to SA simulation and this difference is also comparable to the projected climate change. The choice of domain seems to create a systematic bias in the simulations of temperature and precipitation.

Acknowledgements The authors thank the CORDEX framework, initiated and funded by the World Climate Research Program (WCRP), for providing Rossby centre RCA4 regional climate model data for Middle East North Africa (MENA) and South Asia (SA) regions available at Earth System Grid Federation (ESGF) data portal and hosted at the Swedish Meteorological and Hydrological Institute (SMHI). We also thank the anonymous reviewers for their constructive comments and suggestions.

References

- Abdelmola YK (2009) Surface synoptic type over central Sudan during 1994–2003. PhD Thesis. Department of Meteorology and Climatology, Aristotle University, Thessaloniki, p 404
- Abdullah MA, Al-Mazroui M (1998) Climatological study of the south-western region of Saudi Arabia. I. Rainfall analysis. *Clim Res* 9(3):213–223
- Almazroui M (1998) Climatological study over the southwestern region of the Kingdom of Saudi Arabia with special reference to rainfall distribution, Master thesis, Department of Meteorology, Faculty of Meteorology, Environment and Arid Land Agriculture, King Abdulaziz University, Jeddah
- Almazroui M (2011) Calibration of TRMM rainfall climatology over Saudi Arabia during 1998–2009. *Atmos Res* 99(3–4):400–414. <https://doi.org/10.1016/j.atmosres.2010.11.006>
- Almazroui M (2012) Dynamical downscaling of rainfall and temperature over the Arabian Peninsula using RegCM4. *Clim Res* 52:49–62. <https://doi.org/10.3354/cr01073>
- Almazroui M (2013) Simulation of present and future climate of Saudi Arabia using a regional climate model (PRECIS). *Int J Climatol* 33:2247–2259
- Almazroui M (2016) RegCM4 in climate simulation over CORDEX-MENA/Arab domain: selection of suitable domain, convection and land-surface schemes. *Int J Climatol* 36(1):236–251
- Almazroui M, Islam MN, Jones PD, Athar H, Rahman MA (2012) Recent climate change in the Arabian Peninsula: seasonal rainfall

- and temperature climatology of Saudi Arabia for 1979–2009. *Atmos Res* 111:29–45
- Almazroui M, Abid MA, Athar H, Islam MN, Ehsan MA (2013) Inter-annual variability of rainfall over the Arabian Peninsula using the IPCC AR4 Global Climate Models. *Int J Climatol* 33:2328–2340
- Almazroui M, Nazrul Islam M, Saeed S, Alkhalaf Abdulrahman K, Dambul Ramzah (2017) Assessment of uncertainties in projected temperature and precipitation over the Arabian peninsula using three categories of CMIP5 multimodel ensembles. *Earth Syst Environ* 1:23
- Antic S, Laprise R, Denis B, de Elía R (2004) Testing the downscaling ability of a one-way nested regional climate model in regions of complex topography. *Clim Dyn* 23:473–493
- Attada R, Dasari HP, Chowdary JS, Yadav RK, Knio O, Hoteit I (2018) Surface air temperature variability over the Arabian Peninsula and its links to circulation patterns. *Int J Climatol*. <https://doi.org/10.1002/joc.5821>
- Beck Hylke E, van Dijk Albert IJM, Levizzani Vincenzo, Schellekens Jaap, Miralles Diego Gonzalez, Martens Brecht, de Roo Ad (2017) MSWEP: 3-hourly 0.25° global gridded precipitation (1979–2015) by merging gauge, satellite, and reanalysis data. *Hydrol Earth Syst Sci* 21(1):589–615
- Bergant K, Belda M, Halenka T (2007) Systematic errors in the simulation of European climate (1961–2000) with RegCM3 driven by NCEP/NCAR reanalysis. *Int J Climatol* 27(4):455–472. <https://doi.org/10.1002/joc.1413>
- Bollasina M, Nigam S (2011) The summertime “heat” low over Pakistan/northwestern India: evolution and origin. *Clim Dyn* 37(5–6):957–970
- Bozkurt D, Sen OL (2011) Precipitation in the Anatolian Peninsula: sensitivity to increased SSTs in the surrounding seas. *Clim Dyn* 36(3–4):711–726. <https://doi.org/10.1007/s00382-009-0651-3>
- Buchignani E, Mercogliano P, Panitz HJ, Montesarchio M (2018) Climate change projections for the Middle East-North Africa domain with COSMO-CLM at different spatial resolutions. *Adv Clim Change Res* 9(1):66–80
- Centella-Artola A, Taylor MA, Bezanilla-Morlot A, Martinez-Castro D, Campbell JD, Stephenson TS, Vichot A (2015) Assessing the effect of domain size over the Caribbean region using the PRECIS regional climate model. *Clim Dyn* 44(7–8):1901–1918
- Colin J, Déqué M, Radu R, Somot S (2010) Sensitivity study of heavy precipitation in limited area model climate simulations: influence of the size of the domain and the use of the spectral nudging technique. *Tellus A* 62:591–604. <https://doi.org/10.1111/j.1600-0870.2010.00467.x>
- Dee DP, Uppala SM, Simmons AJ, Berrisford P, Poli P, Kobayashi S, Andrae U, Balmaseda MA, Balsamo G, Bauer P, Bechtold P, Beljaars AC, van de Berg L, Bidlot J, Bormann N, Delsol C, Dragani R, Fuentes M, Geer AJ, Haimberger L, Healy SB, Hersbach H, Hólm EV, Isaksen L, Kållberg P, Köhler M, Matricardi M, McNally AP, Monge-Sanz BM, Morcrette J, Park B, Peubey C, de Rosnay P, Tavolato C, Thépaut J, Vitart F (2011) The ERA-Interim reanalysis: configuration and performance of the data assimilation system. *Q J R Meteorol Soc* 137(656):553–597
- Denis B, Laprise R, Caya D, Côté J (2002) Downscaling ability of one-way nested regional climate model: the Big-Brother Experiment. *Clim Dyn* 18:627–646
- Denis B, Laprise R, Caya D (2003) Sensitivity of a regional climate model to the resolution of the lateral boundary conditions. *Clim Dyn* 20:107–126
- Diaconescu EP, Laprise R, Sushama L (2007) The impact of lateral boundary data errors on the simulated climate of a nested regional climate model. *Clim Dyn* 28(4):333–350
- Dimitrijevic M, Laprise R (2005) Validation of the nesting technique in a regional climate model and sensitivity tests to the resolution of the lateral boundary conditions during summer. *Clim Dyn* 25:555–580
- Evans JP (2009) 21st century climate change in the Middle East. *Clim Change* 92(3–4):417–432
- Evans JP (2010) Global warming impact on the dominant precipitation processes in the Middle East. *Theor Appl Climatol* 99(3–4):389–402
- Fan Y, van den Dool H (2008) A global monthly land surface air temperature analysis for 1948–present. *J Geophys Res* 113:D01103. <https://doi.org/10.1029/2007JD008470>
- Feser F, Rockel B, Storch H, Winterfeldt J, Zahn M (2011) Regional climate models add value to global model data: a review and South-Asian summer monsoon selected examples. *Bull Am Meteorol Soc* 92(9):1181–1192
- Frieler K, Lange S, Piontek F, Reyer CP, Schewe J, Warszawski L, Zhao F, Chini L, Denvil S, Emanuel K, Geiger T (2017) Assessing the impacts of 1.5 C global warming—simulation protocol of the Inter-Sectoral Impact Model Intercomparison Project (ISIMIP2b). *Geosci Model Dev* 10(12):4321–4345
- Gilbert RO (1987) Statistical methods for environmental pollution monitoring. Wiley, New York
- Giorgi F, Bi X (2000) A study of internal variability of a regional climate model. *J Geophys Res Atmos* 105(D24):29503–29521
- Giorgi F, Mearns LO (1999) Introduction to special section: regional climate modeling revisited. *J Geophys Res* 104(D6):6335–6352
- Harris I, Jones PD, Osborn TJ, Lister DH (2014) Updated high-resolution grids of monthly climatic observations—the CRU TS3.10 Dataset. *Int J Climatol* 34(3):623–642. <https://doi.org/10.1002/joc.3711>
- Houghton JT, Ding Y, Griggs DJ, Noguer M, van der Linden PJ, Dai X, Maskell K, Johnson CA (eds) (2001) Climate change. The scientific basis. Contribution of working group I to the third assessment report of the intergovernmental panel on climate change, Cambridge University Press, Cambridge
- IPCC, Collins M, Knutti R, Arblaster J, Dufresne JL, Fichet F T, Friedlingstein P, Gao X, Gutowski WJ, Johns T, Krinner G, Shongwe M, Tebaldi C, Weaver AJ, Wehner M (2013) Long-term climate change: projections, commitments and irreversibility. In: Stocker TF, Qin D, Plattner GK, Tignor M, Allen SK, Boschung J, Nauels A, Xia Y, Bex V, Midgley PM (eds) Climate Change 2013: the physical science basis. Contribution of Working Group I to the Fifth Assessment Report of the Intergovernmental Panel on Climate Change. Cambridge University Press, Cambridge
- Jacob D, Podzun R (1997) Sensitivity studies with the regional climate model REMO. *Meteorol Atmos Phys* 63:119–129. <https://doi.org/10.1007/BF01025368>
- Jones RG, Murphy JM, Noguer M (1995) Simulation of climate change over Europe using a nested regional climate model. Part I: Assessment of control climate, including sensitivity to location of lateral boundaries. *Q J R Meteorol Soc* 121(526):1413–1449
- Jones RG, Murphy JM, Noguer M, Keen AB (1997) Simulation of climate change over Europe using a nested regional climate model. II: comparison of driving and regional model responses to a doubling of carbon dioxide. *Q J R Meteorol Soc* 123(538):265–292
- Kendall MG (1975) Rank correlation methods. Charles Griffin, London
- Leduc M, Laprise R (2009) Regional climate model sensitivity to domain size. *Clim Dyn* 32(6):833–854
- Lioubimtseva E (2004) Climate change in arid environments: revisiting the past to understand the future. *Prog Phys Geogr Earth Environ* 28(4):502–530
- Mann HB (1945) Nonparametric tests against trend. *Econometrica* 13:245–259
- Messenger C, Gallee H, Brasseur O (2004) Precipitation sensitivity to regional SST in a regional climate simulation during the West African monsoon for two dry years. *Clim Dyn* 22(2–3):249–266

- Moss RH, Edmonds JA, Hibbard KA, Manning MR, Rose SK, Van Vuuren DP, Carter TR, Emori S, Kainuma M, Kram T, Meehl GA, Mitchell JFB, Nakicenovic N, Riahi K, Smith SJ, Stouffer RJ, Thomson AM, Weyant JP, Wilbanks TJ (2010) The next generation of scenarios for climate change research and assessment. *Nature* 463(7282):747–756
- Pal JS, Eltahir EAB (2016) Future temperature in Southwest Asia projected to exceed a threshold for human adaptability. *Nat Clim Change* 6:197–200
- Samuelsson P, Jones CG, Willén U, Ullerstig A, Gollvik S, Hansson U, Jansson C, Kjellström E, Nikulin G, Wyser K (2011) The Rossby Centre Regional Climate Model RCA3: model description and performance. *Tellus Ser A* 63(1):4–23
- Schneider U, Becker A, Finger P, Meyer-Christoffer A, Rudolf B, Ziese M (2015) GPCC full data reanalysis version 7.0 at 0.5°: monthly land-surface precipitation from rain-gauges built on GTS-based and historic data. https://doi.org/10.5676/dwd_gpcc/fd_m_v7_050
- Sen PK (1968) Estimates of the regression coefficient based on Kendall's Tau. *J Am Stat Assoc* 63:1379–1389. <https://doi.org/10.1080/01621459.1968.10480934>
- Seth A, Giorgi F (1998) The effects of domain choice on summer precipitation simulation and sensitivity in a regional climate model. *J Clim* 11(10):2698–2712
- Shiao CH, Juang HMH (2006) Sensitivity study of the climate simulation over East Asia with the CWB regional spectral model. *Terr Atmos Ocean Sci* 17(3):593–612
- Sowers J, Vengosh A, Weinthal E (2011) Climate change, water resources, and the politics of adaptation in the Middle East and North Africa. *Clim Change* 104(3–4):599–627. <https://doi.org/10.1007/s10584-010-9835-4>
- Subyani AM (2004) Geostatistical study of annual and seasonal mean rainfall patterns in southwest Saudi Arabia/Distribution géostatistique de la pluie moyenne annuelle et saisonnière dans le Sud-Ouest de l'Arabie Saoudite. *Hydrol Sci J*. <https://doi.org/10.1623/hysj.49.5.803.55137>
- Syed FS, Iqbal W, Syed AAB, Rasul G (2014) Uncertainties in the regional climate models simulations of South-Asian summer monsoon and climate change. *Clim Dyn* 42:2079–2097
- Tanarhte M, Hadjinicolaou P, Lelieveld J (2012) Intercomparison of temperature and precipitation data sets based on observations in the Mediterranean and the Middle East. *J Geophys Res* 117:D12102. <https://doi.org/10.1029/2011JD017293>
- Taylor KE (2001) Summarizing multiple aspects of model performance in a single diagram. *J Geophys Res Atmos* 106(D7):7183–7192
- Taylor KE, Stouffer RJ, Meehl GA (2012) An overview of CMIP5 and the experiment design. *Bull Am Meteorol Soc* 93(4):485–498
- Willmott CJ, Matsuura K (2001) Terrestrial air temperature and precipitation: monthly and annual time series (1950–1999) version 1.02. Center for Climatic Research, University of Delaware, Newark
- Wu W, Lynch AH, Rivers A (2005) Estimating the uncertainty in a regional climate model related to initial and lateral boundary conditions. *J Clim* 18(7):917–933
- Xie PP, Chen M, Shi W (2010) CPC unified gauge-based analysis of global daily precipitation. Preprints, 24th Conference on Hydrology, Atlanta, GA. Amer Meteor Soc 2.3A. http://ams.confex.com/ams/90annual/techprogram/paper_163676.htm
- Zhang X, Aguilar E, Sensoy S, Melkonyan H, Tagiyeva U, Ahmed N, Kutaladze N, Rahimzadeh F, Taghipour A, Hantosh TH, Albert P (2005) Trends in Middle East climate extreme indices from 1950 to 2003. *J Geophys Res Atmos* 110:D22. <https://doi.org/10.1029/2005JD006181>
- Zittis G (2018) Observed rainfall trends and precipitation uncertainty in the vicinity of the Mediterranean, Middle East and North Africa. *Theor Appl Climatol* 134:1207–1230

Publisher's Note Springer Nature remains neutral with regard to jurisdictional claims in published maps and institutional affiliations.